Energy & Buildings 358 (2026) 117192

Contents lists available at ScienceDirect

Energy & Buildings

journal homepage: www.elsevier.com/locate/enb

RHpT: Bioclimatic framework for passive climate-adaptive bio-façades in urban contexts☆

Kumar Biswajit Debnath [a,c,*], Natalia Pynirtzi [b], Jane Scott [a], Colin Davie [b], Ben Bridgens [a]

[a] Hub for Biotechnology in the Built Environment, School of Architecture, Planning and Landscape, Newcastle University, Newcastle Upon Tyne NE1 7RU, United Kingdom
[b] School of Engineering, Newcastle University, Newcastle Upon Tyne NE1 7RU, United Kingdom
[c] School of Architecture, University of Technology Sydney, Sydney, NSW 2007, Australia

ARTICLE INFO

Keywords:
Bio-climatic framework
Material testing
Responsive bio-based material
Bio-façade
Cooling energy demand

ABSTRACT

Globally, cities are grappling with intensifying heat stress and rising cooling energy demand, with the impacts disproportionately falling on populations in the Global South, where access to adaptive technologies remains limited. We present 'Relative Humidity–Temperature Profiling (RHpT)', a scalable climatic screening framework that identifies windows of opportunity in which humidity-responsive materials can enable passive, sensor-free building adaptation. Using two climatically distinct cities (New Delhi and Newcastle upon Tyne), we show that RHpT can identify seasonal and diurnal conditions suitable for actuation, and that these are validated through laboratory characterisation of larch veneers and dynamic building simulations. In non-optimised retrofit scenarios, RHpT-guided façades reduced cooling demand by up to 10%. More broadly, RHpT offers a transferable method for cities to assess the feasibility of bio-based adaptive envelopes, connecting climate logic to material thresholds and energy outcomes. This approach demonstrates how bio-responsive, low-cost design strategies can contribute to just and low-carbon urban resilience.

1. Introduction

Megacities and dense urban areas across the Global South are epicentres of the climate crisis, where rapid urbanisation, combined with the urban heat island effect, intensifies thermal stress [1,2] and makes active cooling solutions a necessity for survival, yet often an unaffordable luxury [3,4]. In these contexts, rising cooling demand coincides with limited access to mechanical cooling, unreliable energy infrastructure, and constrained capacity for maintenance and system management [3,5]. Retrofitting existing urban buildings—often characterised by high density, limited façade access, and informal construction—poses additional challenges that make energy-dependent or sensor-driven adaptive façade technologies difficult to deploy at scale [6]. Furthermore, while various passive and smart building skin technologies have emerged, from traditional vernacular designs [7] to sophisticated adaptive systems [8], many rely on materials with high embodied energy, are energy-dependent, or utilise rare earth materials extracted through environmentally and socially problematic practices [9–11].

This creates an urban design challenge: how can building skins in these resource-constrained settings passively respond to temperature fluctuations using locally available, biodegradable materials, without the need for sensors, power, or mechanical components? Humidity-responsive (hygromorphic) bio-based materials, such as wood [12–14], bacterial cellulose [15], and mycelium-based composites [16,17], offer a promising pathway, as they respond anisotropically to changes in relative humidity (RH), enabling climate-driven actuation through natural expansion and contraction. Thin wood veneers (0.6–1.0 mm thick), for example, can deflect visibly within minutes of RH shifts, offering a passive, reversible mechanism to open or close ventilation apertures without electronics or user input [18]. These bio-based materials are not only abundant and biodegradable but also exhibit passive behaviour well-matched to daily climatic rhythms, offering immense potential to enhance building performance and sustainability.

Previous research has demonstrated the architectural feasibility of wood bilayer actuators and other hygroscopic systems. Several studies explored the design and application of humidity-responsive bio-based materials in adaptive building façades. Reichert, S. et al. (2015)

☆ This article is part of a special issue entitled: 'ENB_Rethinking Passive Energy' published in Energy & Buildings.

* Corresponding author.
E-mail address: KumarBiswajit.Debnath@uts.edu.au (K.B. Debnath).

https://doi.org/10.1016/j.enbuild.2026.117192
Received 24 October 2025; Received in revised form 20 January 2026; Accepted 18 February 2026
Available online 19 February 2026

developed a 'Meteorosensitive architecture' with a biomimetic, responsive building skin that adapts to environmental changes through hygroscopic material properties [19]. Rüggeberg and Burgert (2015) developed bio-inspired actuators to demonstrate the actuation of wooden bilayers in response to changes in relative humidity [20]. Holstov, A. et al. (2015) designed adaptive building systems based on bilayer hygromorphic composites with wood as the active layer to passively regulate the variable natural rhythms of the internal and external environments [18]. Menges, A. and Reichert, S. (2015) demonstrated the architectural potential of hygroscopically actuated wood through advanced design computation and digital fabrication [21]. Wood, D. M. et al. (2016) presented an upscaling of a hygroscopically actuated timber-based system for self-constructing building surfaces [22]. Poppinga S. et al. (2017) reported, among others, a humidity-responsive bi-layer flap system comprising rubber and hydrogel, with potential applications in architecture [23]. Grönquist, P. et al. (2018) propose a simple 2D linear elastic model for predicting the curvature of thin wooden bilayers as a function of moisture change, accounting for moisture-dependent orthotropic wood properties and a physically accurate reduction to 2D [24]. Vailati, C. et al. (2018) developed a combination of two wood bilayers as a possible solution for implementing shading elements [25]. Another study by Grönquist, P. et al. (2019) proposed an efficient form-giving mechanism for large-scale curved mass timber using bilayered wood structures that self-shape due to changes in moisture content [26]. Pelliccia, G. et al. (2020) developed and characterised timber panels for adaptive hygrothermal comfort with passive dehumidification in indoor environments [27]. Grönquist et al. (2020) propose using self-shaping wood bilayer strips in grid-shell configurations to achieve double curvature through a parametric phase space of shaping, as determined by numerical mechanical simulations [28]. El-Dabaa, R. et al. (2021) designed a framework for programmable actuation in an adaptive building façade using hygroscopic wood and its passive response to fluctuations in relative humidity [29]. Yet, these studies have focused mainly on material mechanics and fabrication, without establishing clear links between local climatic conditions and the operational viability of these systems. A fundamental barrier to broader adoption is the absence of a climate-driven framework to determine where and when these materials can perform effectively.

The bioclimatic approach comprises six stages: climate data, evaluation, calculation methods, findings, practical considerations, and synthetic application [30], in which climate data would become the basis for architectural applications. In the studies mentioned above, the objective of exploring or enhancing material properties guided the design, without a contextual, weather- or climate-specific approach. Neglecting architectural application requirements in material development for building skin use was often proven to be a failure in achieving the desired outcome [31]. In experiments and characterisation of bio-based hygroscopic materials for building applications, one significant challenge was the lack of a methodology to specify the appropriate relative humidity and temperature ranges. This was necessary for developing and calibrating the materials for year-round, seasonal, monthly, or daily applications. Additionally, given the scarcity of thermoresponsive bio-based materials, it may be worthwhile to explore the use of abundant humidity-responsive bio-based materials for responsive facade applications. This is due in part to the absence of a generalisable method for matching material behaviour to local climatic conditions [18,32–34]. Most studies emphasise material properties over architectural context [30,31,35,36], resulting in a lack of climate-specific guidance on the use of hygromorphic materials in buildings [18].

In this study, we introduce the 'Relative Humidity–Temperature Profiling (RHpT)' method: a bioclimatic framework that leverages long-term weather data to identify when and where RH can serve as a reliable surrogate for temperature, thus enabling passive material actuation. While the inverse relationship between air temperature and relative humidity is well established in atmospheric science and thermodynamics, this study's contribution does not lie in redefining or rediscovering this physical relationship. RHpT does not introduce a new climatic variable, nor does it aim to predict vapour pressure, moisture flux, or psychrometric behaviour. Instead, RHpT operationalises the temporal reliability of the humidity–temperature relationship for architectural design. By identifying specific seasonal and diurnal windows during which relative humidity consistently covaries with cooling-relevant temperature states, the framework enables humidity to function as a practical substitution for temperature in passive, material-driven actuation. In this sense, RHpT is a design-oriented screening method that connects long-term climate data to material thresholds and façade operation logic, rather than a new thermodynamic model. We apply this method in two climatically distinct cities—New Delhi, India and Newcastle upon Tyne (hereafter referred to as Newcastle), UK—to generate RHpT operational thresholds. These climate insights are then validated through laboratory testing of larch veneer and building-scale simulation of a responsive façade system (Bio-HNV). This study uses ambient data as a first step to establish a foundational understanding of the climate-specific relationship between RH and T, providing initial design thresholds for material characterisation.

Together, the RHpT method, material characterisation, and dynamic thermal simulation form a low-cost, circular, and climate-attuned strategy that directly contrasts with conventional smart façades, which often depend on energy, sensors, or rare-earth materials. Unlike fixed passive systems, this triad offers a dynamic, self-regulating solution utilising abundant bio-based materials and climate-responsive logic, providing operational advantages in low-resource settings where smart infrastructure is infeasible. This approach is particularly well-suited for retrofitting buildings in hot-humid climates with limited access to energy or smart infrastructure, enabling sensor-free passive cooling.

Within the urban context, passive and self-regulating building envelope strategies offer a critical alternative. Humidity-responsive bio-based materials are particularly relevant for cities where daily and seasonal climatic rhythms are pronounced, as they can enable adaptive behaviour without external energy input, sensors, or user control. However, their effective application in urban environments requires understanding when local climate conditions reliably trigger beneficial responses, especially in the complex, variable microclimates of cities. The RHpT framework is developed explicitly to address this gap. By analysing long-term, city-scale climatic data, RHpT identifies temporal windows during which relative humidity can serve as a reliable alternative for temperature, enabling passive actuation logic suited to dense urban settings. Rather than optimising individual buildings in isolation, RHpT provides a scalable screening approach that supports climate-responsive retrofit strategies across urban building stocks, particularly in resource-constrained cities where low-cost, low-maintenance solutions are essential.

2. Materials and methods

This study was part of an interdisciplinary project, RESPIRE (Passive, Responsive, Variable Porosity Building Skins), in which bioclimatic design and material engineering collaborated. Within the bioclimatic design approach, parameters such as air temperature, relative humidity, and absolute humidity were analysed using long-range historical data, combined with lab-based material characterisation and dynamic simulations to analyse thermal comfort and cooling demand, and to develop temperature and humidity ranges. These ranges guided the development of experimental materials and characterisation for creating bio-based passive and adaptive building façades.

2.1. Climate analysis

Two cities (New Delhi, India, and Newcastle upon Tyne, UK) with temperate climates, according to the Köppen-Geiger system [37], were selected to analyse the relationship between relative humidity and air

temperature. Typical meteorological year (TMY) climate data from 2004 to 2018 were obtained from [38] for the climate analysis.

2.2. Weather data analysis

Furthermore, weather data from 37 years (January 1, 1985-November 23, 2022) was provided by Meteoblue (www.meteoblue.com). The metadata were called European Centre for Medium-Range Weather Forecasts (ECMWF) Reanalysis 5th Generation (ERA5, ERA5T), with a spatial resolution of 30 km and an Hourly temporal resolution. According to Meteoblue [39]: The ERA5 dataset was generated utilising 4DVar data assimilation within the CY41R2 version of the European Centre for Medium-Range Weather Forecasts (ECMWF) Integrated Forecast System (IFS). It comprises 137 hybrid sigma/pressure levels in the vertical dimension, with the top-level positioned at 0.01 hPa. Atmospheric data is available at these levels and is further interpolated to 37 pressure levels, 16 potential-temperature levels, and 1 potential-vorticity level. Additionally, "surface or single level" data is available, encompassing two-dimensional parameters such as precipitation, 2-meter temperature, top-of-atmosphere radiation, and vertical integrals across the entire atmosphere. It is important to note that the ERA5T data covering the period from 1940 to 1980 exhibits reduced accuracy due to the absence of satellite observations before 1980.

We used the Pearson correlation (coefficient and p-value) for the relationship analysis of the weather data. The Pearson coefficient and p-value were interpreted together to evaluate the significance of the relationship [40]. The relationship was statistically significant when the coefficient was close to + 1.0, and the p-value was less than 0.05. Satisfying only one was considered a statistically insignificant relationship. We used Python for data and statistical analysis, utilising libraries such as Pandas, NumPy, Matplotlib, SciPy, and CSV.

The ECMWF Reanalysis 5th Generation dataset played a pivotal role in our analysis. However, it is imperative to acknowledge that the estimation process involved assumptions, inaccuracies, and uncertainties, as extensively detailed in [41,42]. These factors introduce nuance and potential variability that could affect the accuracy and reliability of the results.

2.3. RHpT method

The RHpT method's plots were created with 37 years (1985–2022) of data collectively for four temporal scales: (1) All data collectively, (2) Day and night, (3) Summer and winter day and night, and (4) monthly day and night. The summer season was from April to September, and the winter season was from October to March. Moreover, 6 am-6 pm was considered Day and 7 pm-5 am was Night. The RHpT plots were created using Python and various libraries, including Pandas, NumPy, Matplotlib, SciPy, Scikit-learn, Statsmodels, and CSV (Supplementary code). First, the data was sliced into the required time frames: summer, winter, monthly, day, and night. Then, all the hourly temperature and relative humidity data were plotted in a correlation plot with a linear regression line, using the required temporal scale. Then, the regression lines were plotted using their corresponding line equations and R-squared values. The regression lines were presented with 80% and 95% confidence intervals. The monthly correlation plot was presented with only the regression lines, equations, and R-squared values to reduce the number of crowded subplots. We assessed the thermal comfort range for the temperatures against the India Model for Adaptive Comfort (IMAC), which suggested that the neutral temperature in naturally ventilated buildings ranged from 19.6 to 28.5 °C [43]. The heating zone was considered below 19.6 °C, and the cooling zone was above 28.5 °C.

2.4. Material testing of humidity-responsive wood veneer

To validate the RH actuation potential suggested by the RHpT analysis, we conducted laboratory tests on humidity-responsive wood veneers. We introduced the Bio-based Humidity-responsive Night Ventilation (Bio-HNV) system, consisting of a single layer of wood veneers. In this system, individually anchored veneer strips deflect under higher relative humidity than that at which they were secured (Fig. 1A). Arranged in a woven pattern, these strips form a screen that utilises the wood's response to humidity changes to enable night ventilation. Various wood types, grain directions, weave patterns, and fabrication conditions were tested to provide proof-of-concept evidence of specific air permeability at set humidity levels. Scottish larch was chosen for its dimensional stability, low cost, and proven responsiveness to changes in ambient moisture. As a durable, locally sourced softwood primarily used for external cladding in the UK, it readily absorbs and releases moisture, with tangential and radial expansion coefficients of 9.1% and 4.5%, respectively [44]. Primarily used for external cladding, Scottish larch is a durable, locally sourced option in the UK. Its features made it suitable for this work. The selection of larch veneers was based on their dimensional stability, low cost, and proven responsiveness to changes in ambient moisture. The tests aimed to define the material's RH-actuation thresholds, helping to assess whether the RH ranges identified by RHpT align with real-world material responses.

In this study, we developed a small prototype using a 6 mm-thick, 180 mm x 180 mm plywood panel and a 0.6 mm-thick Scottish larch veneer sheet. Nine rectangular veneer strips, 160 mm long and 30 mm wide, were laser-cut with grain perpendicular to the cut for maximum deflection at high humidity. These strips were bolted to a 180 mm x 180 mm plywood panel with 2 mm bolts spaced 20 mm apart, featuring a 150 mm x 150 mm aperture (Fig. 1B and C).

A large-scale prototype was developed to evaluate the performance of the small-scale version, featuring 1 mm (thickness) Scottish larch strips (8.2 mm wide and 44 mm long) bolted onto a 6 mm (thickness), 600 mm x 600 mm plywood panel, which included a 500 mm x 500 mm aperture opening. Both setups were placed in a climate chamber maintained at 25 °C. The small-scale tests varied RH at 4 levels —20%, 50%, 70%, and 90% — to assess the larch's moisture responsiveness. For the large-scale tests, the RH range was reduced to 20%-70% to match the climatic conditions in New Delhi, and the RHpT was analysed. Previous experiments have shown that temperature has a minimal impact, emphasising the importance of focusing on RH variations relevant to New Delhi.

2.4.1. Deflection measurements

The out-of-plane deflection of the larch veneers was measured manually using an RS PRO Digital Calliper with an accuracy of 0.1 mm. The maximum deflection was observed at the centre of the panel. The deflection from the panel surface to the highest deflection point was measured to ensure accuracy. Three deflection measurements were taken at different locations around the panel's centre. The exact locations were measured each time, and the results were reported as the average of these three measurements.

2.4.2. Cyclic tests

The small-scale cyclic tests lasted for five consecutive days, with each cycle lasting 4 hours (h). The first cycle commenced at an RH of 20%, during which the woven structure was maintained for 1 h. During the wetting process, the RH was set to 50% for 1 h, then increased to 70% for another 1 h. The drying followed the exact pattern until the RH settings were back to 20%. Adjusting the RH settings in the climate chamber takes approximately 10 min for the system to reach equilibrium at the desired RH level. Deflection measurements of the Bio-HNV were taken every 10 min for 30 min, then again at 1 h. The next cycle would start when the Bio-HNV remained at 20% RH for 1 h. The first two cycles are shown in Fig. 7B.

2.4.3. Scalability and unit-cell behaviour

The tested veneer samples (150 mm x 150 mm and 500 mm x 500 mm) are intended to characterise the material's intrinsic hygromorphic

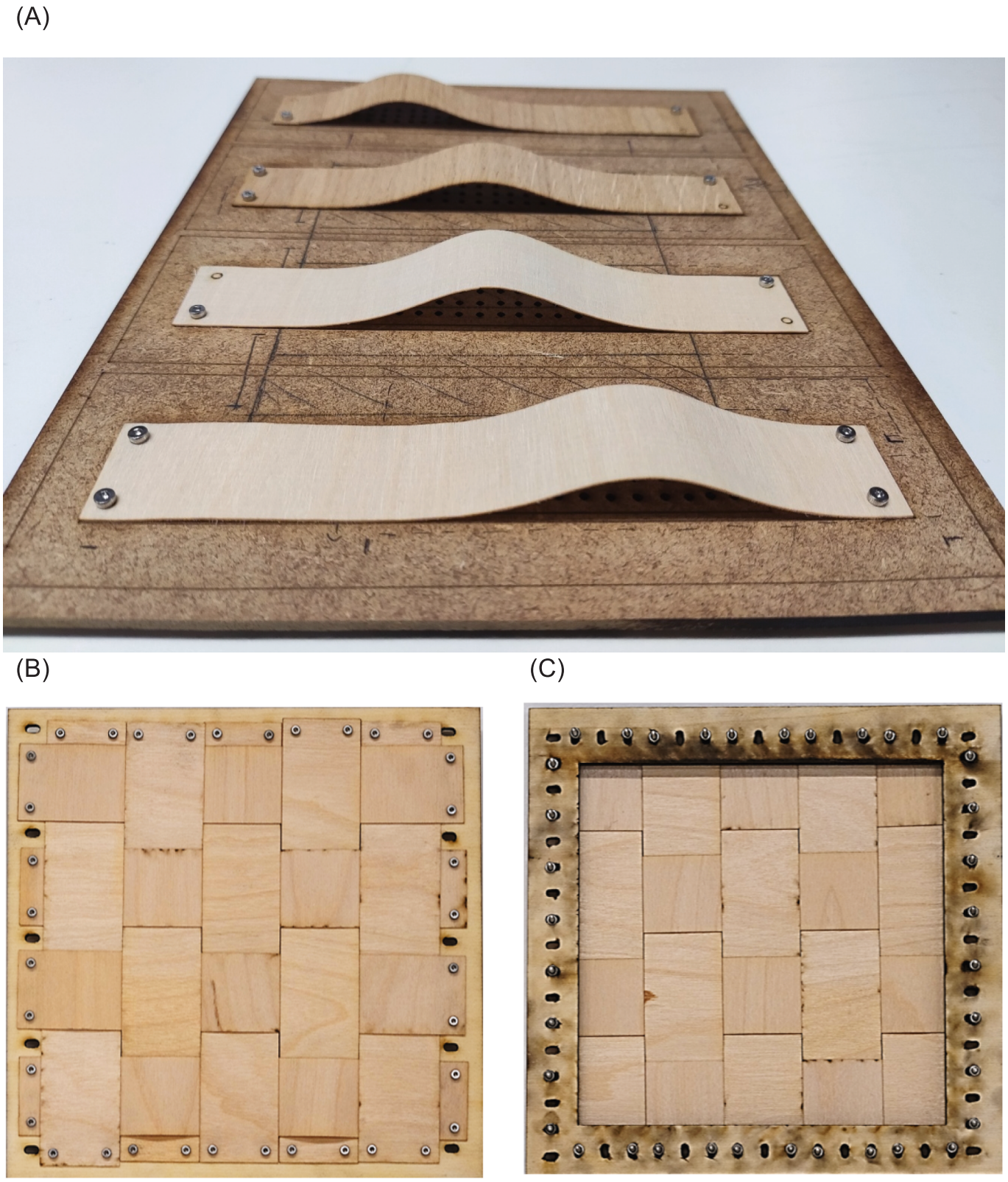

Fig. 1. (A) Single-layer system of larch veneer strips, fixed at both ends, deflecting at RH = 90%. Bio-HNV small-scale prototype (B) front, (C) back of the panel. Overall panel size 180 mm x 180 mm, window size = 150 mm x 150 mm, strip width 30 mm, strip length = 160 mm, strip thickness 0.6 mm.

response at the unit scale, rather than to represent full-size building apertures. In architectural applications, humidity-responsive façades are typically realised as arrays of modular elements, where global behaviour emerges from the repetition of locally responsive units rather than from a single continuous opening. As such, the measured curvature, opening angles, and response times are expected to remain qualitatively consistent at larger scales, while absolute deformations and airflow rates would depend on module size, framing, and façade integration.

Non-linear scaling effects related to structural stiffness, wind pressure, and coupled airflow across multiple modules are not captured in the present experiments and remain an important subject for future façade-scale testing and numerical analysis. Accordingly, the results presented here should be interpreted as material-level and component-level performance indicators, rather than direct predictors of full-building aperture behaviour.

2.4.4. Material durability, fatigue, and environmental ageing

The experimental programme presented here is intentionally limited to short-term, material-level characterisation of hygromorphic responsiveness under controlled humidity cycles. The cyclic chamber tests are designed to establish actuation thresholds, reversibility, and qualitative response trends, rather than to assess long-term durability, fatigue, creep, or environmental ageing under real outdoor exposure.

Long-term performance aspects—including mechanical fatigue under repeated humidity cycling, creep deformation under sustained loading, ultraviolet exposure, biological degradation, and surface weathering—are critical considerations for façade-scale deployment but fall outside the scope of this proof-of-concept study. In the RHpT workflow, such durability testing constitutes a second-phase validation step following climate suitability screening and initial material qualification.

2.5. Building simulation of Bio-HNV façade performance

The operation and practicalities of retrofitting the Bio-HNV systems were tested using the dynamic building simulation software DesignBuilder and EnergyPlus to evaluate their performance in terms of indoor operative temperature and cooling energy demand on a building-scale retrofit. For the Base case, a single-zone indoor office space (100 m^2) was modelled (Fig. 2A) in DesignBuilder, with dimensions of 10 m in length, 10 m in width, and 3.5 m in height. The construction and materials used are described in Table 1. A window (2.7 m x 1.2 m) with single-layer clear glass and a horizontal shading lentil on the South façade. There was an air-conditioning (AC) unit — a fan coil unit (4-Pipe) — and an air-cooled chiller operating at 100% capacity (in summer) in the office, which operates during office hours from 9 am to 5 pm. The AC unit operated at 25% from 7:00 to 8:00 am, reaching 50% by 9:00 am. The AC unit operated at 75% (capacity) during lunch, from 12:00 p.m. to 2:00 p.m. Additionally, the AC unit began operating at 50% capacity between 5:00 and 6:00 p.m., and by 6:00 p.m., its capacity had decreased to 25%. The AC unit was not operating outside office

Table 1
Construction name, thickness, and materials; for the material properties, we used a software database.

Name	Thickness (m)	Materials	U-Value (W/m^2-K)
Exterior walls	0.280	Brick wall with cement plaster on both sides	1.977
Ground floor	0.925	Solid basement ground floor, uninsulated	1.066
Flat roof	0.200	Concrete slab	2.422
Glass window	0.003	Single-layer Glass windows	5.894

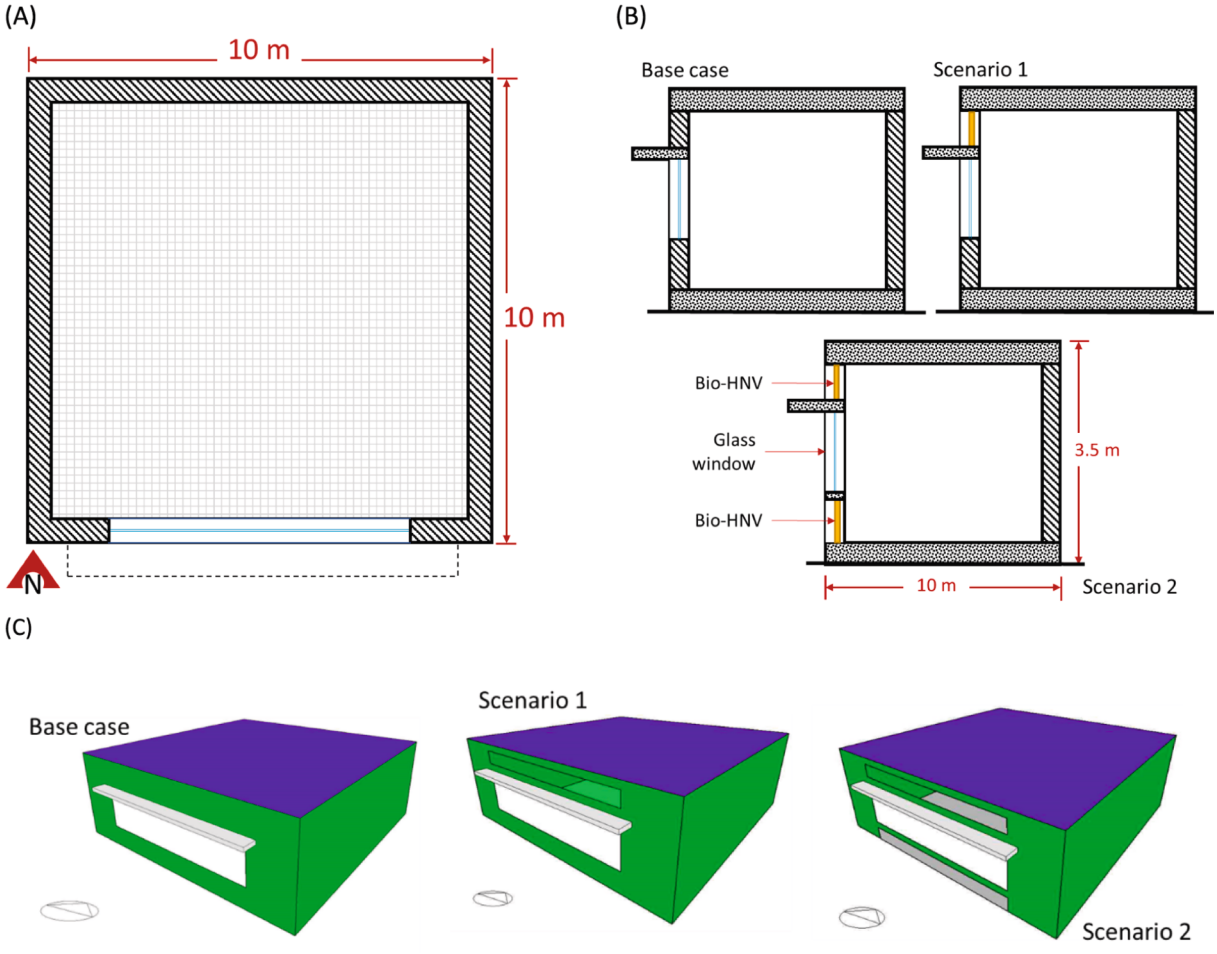

Fig. 2. A) Plan of the simulation space, B) Section and C) Designbuilder model of Base case, Scenario 1 and 2. The drawings are not to scale.

hours, on weekends, or on holidays. The set point temperature for the AC unit was 26 °C, and the cooling setback was 28 °C. There was no night ventilation under the Base case. We used the 'Generic office template' and 0.1110 people/m^2 for the activity template. Additionally, we utilised office equipment with a power density of 11.77 W/m^2. While simulating, we created an adiabatic component around the simulation zone's east, north and west sides to expose only the south wall to the outdoors.

The base case features only the window on the South façade, whereas Scenario 1 (Fig. 2B and C) includes Bio-HNV panels above the window, and Scenario 2 features Bio-HNV panels both above and below the window on the south façade. For both scenarios, the AC unit and Bio-HNV operated under three distinct morning start schedules for the AC: 7:00 a.m., 8:00 a.m., and 9:00 a.m.

- **7:00 a.m. AC Start:** AC operated as in the base case. Bio-HNV was operational from 7:00 p.m. to 7:00 a.m.
- **8:00 a.m. AC Start:** AC began at 25% capacity until 9:00 a.m., reaching 50% by 10:00 a.m., and then followed the base case schedule (75% during lunch, 50% from 5:00–6:00 p.m.). Bio-HNV was operational after office hours (6:00 p.m. – 8:00 a.m.) at 100% capacity.
- **9:00 a.m. AC Start:** AC began at 25% capacity until 10:00 a.m., reaching 50% by 11:00 a.m., and then followed the base case schedule (75% during lunch, 50% from 5:00–6:00 p.m.). Bio-HNV was operational after office hours (6:00 p.m. – 9:00 a.m.) at 100% capacity.

Two temporal analyses were conducted to evaluate the impact of Bio-HNV on the indoor operative temperature and cooling energy demand. First, we selected three summer dates (April 1, July 1, and September 2) to evaluate the impact on hourly indoor operative temperatures. Secondly, we analysed the effect of Bio-HNV on total summer cooling energy demand (April 1-September 30). Weather data from the same historical dataset used in the RHpT study was applied. The IMAC model was used to assess thermal comfort performance [43].

The building-scale simulations presented in this study are intended as illustrative, order-of-magnitude assessments rather than as fully validated performance predictions. Current whole-building energy simulation tools, including EnergyPlus, do not support direct hygro-mechanical modelling of humidity-driven material deformation. As a result, the physical opening of the hygromorphic veneer elements is represented through equivalent free-aperture fractions derived from experimentally observed deformation ranges. These aperture fractions were not optimised to maximise performance, nor calibrated against measured building data, but were instead conservatively selected to reflect non-optimised retrofit conditions. The purpose of the simulation is therefore to explore whether RHpT-informed passive actuation can plausibly influence cooling energy demand, rather than to predict absolute savings or to validate a specific façade configuration.

3. Results and discussion

3.1. From climate data to design strategy

3.1.1. Climate analysis

The analysis of hourly climate data, relative humidity (RH), absolute humidity (AH), and air temperature (T) across a 24-hour cycle revealed that the annual RH and T exhibited substantial fluctuations, ranging from 10—100% and 3.6—44 °C, respectively, in New Delhi (Fig. 3A). Notably, a distinct pattern emerged throughout the year, with an inverse relationship between average RH and T during the day (6 am—6 pm) and night (7 pm—5 am). Daytime showed a decrease in RH accompanied by an increase in T across all months, while nighttime showed a rise in RH accompanied by a decline in T. In New Delhi, the daily fluctuation range in RH and T became narrower during the summer months (June to September) due to consistently high baseline RH and T. However, in the case of Newcastle upon Tyne, the annual variation in RH and T ranged from 30% to 100% and −10 °C to + 24 °C, respectively (Fig. 3B). Unlike New Delhi, Newcastle displayed less pronounced changes in RH and T, except during the summer months.

The AH analysis over the 24 h revealed comparatively minor fluctuations in both New Delhi and Newcastle, especially when contrasted with the more noticeable variations in RH and T (Fig. 3). The daily fluctuation range in RH and T increased from April to September during the summer months, though not as significantly as in New Delhi. Therefore, the subsequent inquiry delved only into whether changes in RH and T co-occurred, a phenomenon that was not conclusively evident in the TMY dataset. To unravel this intricate relationship, an in-depth examination of hourly weather data was conducted in the following section to identify time-dependent correlations among these crucial climate parameters.

3.1.2. Weather analysis

The 37 years of hourly weather data were analysed to investigate the correlation between RH and T in two distinct locations: New Delhi and Newcastle. To provide a nuanced understanding, the correlation analysis focused on 1985, 2003 and 2021, representing the dataset's start, middle and end with complete annual information (Supplementary Table 1 and Fig. 4). Furthermore, we analysed the statistical correlations between RH and T in decadal timeframes: 1985–1994, 1995–2004, 2005–2014, and 2015–2021 (Supplementary Table 2 and Fig. 4). The inverse correlation observed between air temperature and relative humidity in the analysed datasets reflects a well-known thermodynamic relationship. Accordingly, these results should not be interpreted as a novel climatic finding. Rather, the significance of the analysis lies in quantifying the strength, consistency, and temporal structure of this relationship across seasons and diurnal cycles, which enables the identification of specific periods during which humidity-responsive materials can be expected to operate reliably without active control. These correlations are therefore interpreted not as novel climatic findings, but rather as quantitative evidence for identifying reliable actuation windows for humidity-responsive materials.

The decadal analysis of all months also revealed a statistically significant negative correlation between RH and T in New Delhi. Notably, the p-values were consistently below 0.01 throughout the years. All months showed a substantial coefficient value below −0.500 for New Delhi (Supplementary Table 2 and Fig. 4A). The highest correlation coefficients were −0.921, −0.939, −0.949, and −0.947 for the periods 1985–1994, 1995–2004, 2005–2014, and 2015–2021, respectively. The highest correlation coefficients were in August (1985–1994 and 1995–2004), and in July (2005–2014 and 2015–2021). The three-year analysis findings revealed intriguing patterns in New Delhi, where most months exhibited a statistically significant negative correlation between RH and temperature (Supplementary Fig. 1A). Notably, the p-values were consistently below 0.01 throughout the year. While the coefficient was below −0.500 in October 1985 and May 2003, all other months displayed a substantial coefficient value (> −0.500) for New Delhi (Supplementary Table 1 and Fig. 4A). The highest correlation coefficients were −0.921, −0.968 and −0.948 for 1985, 2003 and 2021, respectively. The highest correlation coefficients were observed in August (1985 and 2003), and this trend continued into September 2021.

On the other hand, the relationship between RH and T for Newcastle did not demonstrate a correlation (Supplementary Fig. 1) and statistical significance, except during certain summer months (Fig. 4). The three-year analysis revealed a comparatively weaker, statistically significant negative correlation between RH and T in Newcastle than in New Delhi (Supplementary Fig. 1A). A moderate negative correlation coefficient (Around −0.500) between RH and T was found in Newcastle in May, June, August, and October in 1985, March, June, July, and September in 2003, and May—September 2021 (Supplementary Table 1 and Fig. 4B), except for January and December, which showed positive coefficient

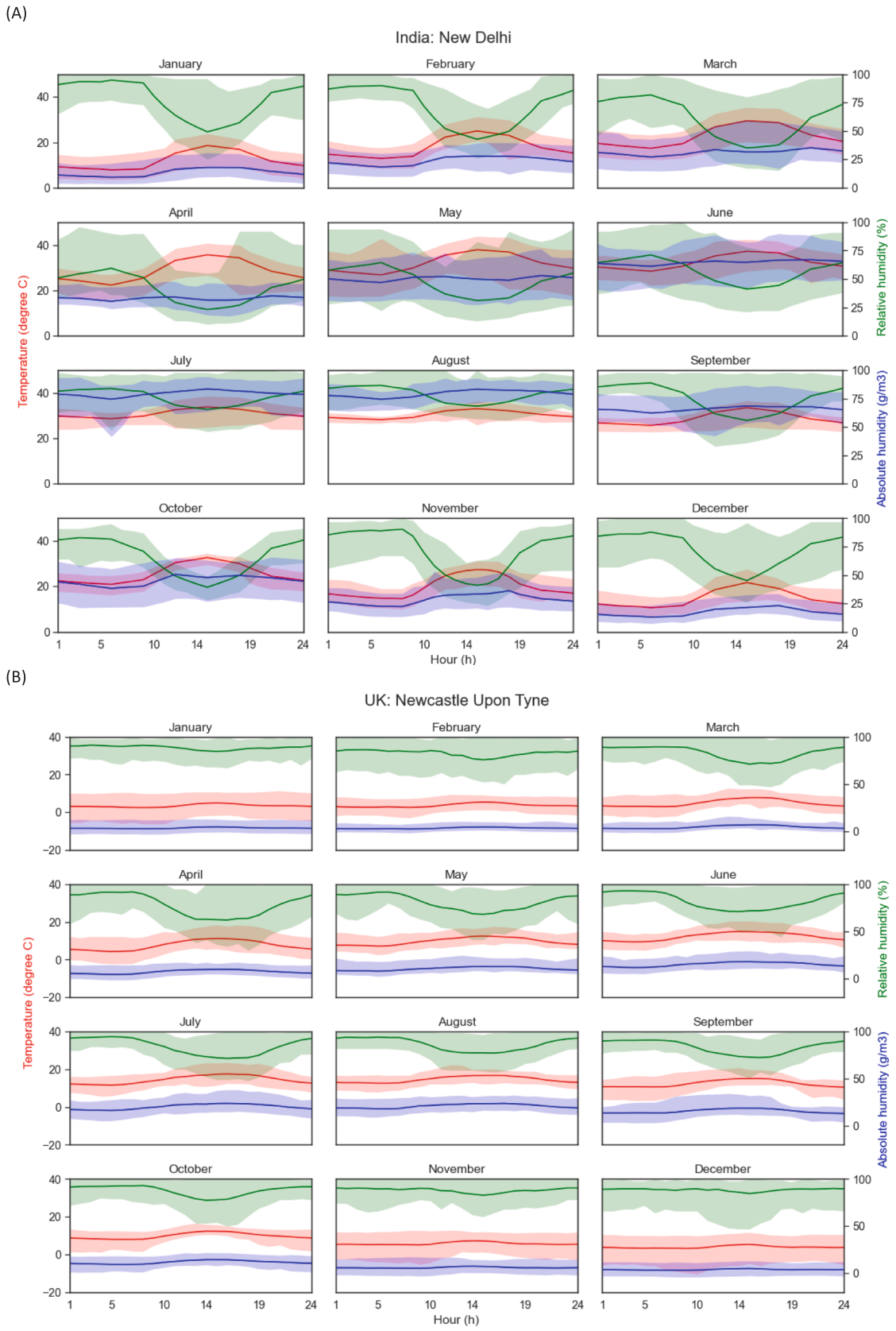

Fig. 3. Hourly Temperature, Absolute and Relative humidity analysis for every month based on TYM data for 2004–2018 in (A) New Delhi, India and (B) Newcastle Upon Tyne, UK.

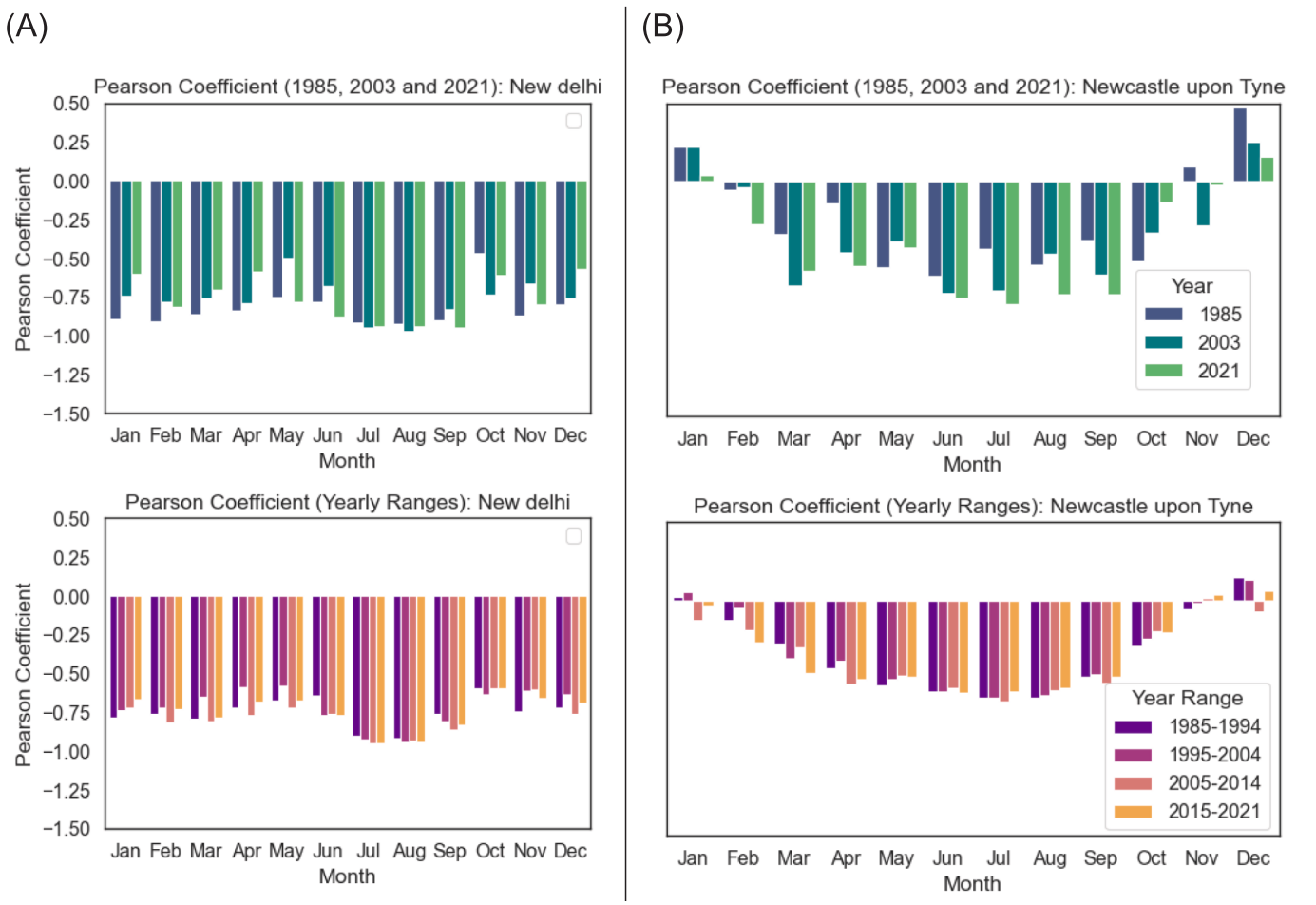

Fig. 4. Pearson coefficient for 1985, 2003, and 2021 (denoting the start, mid, and end years of the dataset) and decadal range (1985–1994, 1995–2004, 2005–2014, and 2015–2021) for (A) New Delhi and (B) Newcastle upon Tyne.

values (Fig. 4). The highest correlation coefficients were −0.599, −0.710 and −0.784 for 1985, 2003 and 2021, respectively. The highest correlation coefficients were in June (1985 and 2003) and July 2021. Furthermore, the p-values were mainly below 0.01, except for February (1985 and 2003) and January and November (2021). The decadal analysis of all months also exhibited a lower statistically significant negative correlation between RH and T in Newcastle. The p-values were mainly below 0.01 throughout the years except for January (1985–1994 and 2015–2021) and November (1995–2004 and 2005–2014) (Supplementary Table 2). All months displayed a substantial coefficient value lower than −0.500 for Newcastle, except for January, November and December (Supplementary Table 2 and Fig. 4A). The highest correlation coefficients were −0.620, −0.619, −0.645, and −0.589 for the periods 1985–1994, 1995–2004, 2005–2014, and 2015–2021, respectively. The highest coefficients were in July (1985–1994, 1995–2004, 2005–2014) and June (2015–2021).

3.1.3. RHpT plot: New Delhi

The relatively low coefficients of determination (R^2) observed when analysing long-term, all-hours datasets reflect the inherent climatic variability present across seasons, diurnal cycles, and weather regimes. In the context of RHpT, a high global R^2 is not the primary objective. Instead, the framework focuses on identifying temporally constrained periods—such as summer daytime or night-time windows—during which the humidity–temperature relationship becomes sufficiently consistent to support reliable passive actuation. This is evidenced by the substantially higher R^2 values observed in seasonal and monthly subsets, which are more relevant to architectural operation.

Due to relatively significant statistical correlations, we developed RHpT plots for New Delhi. First, all the RH (Y-axis) and T (X-axis) data for 1985–2022 were plotted in a correlation plot, which included 332,184 data points (Fig. 5A). The estimated regression line yielded a coefficient of determination (R^2) value of 0.20, as shown in Eq. (1). Fig. 5A also shows the estimated regression's 80% and 95% confidence bands. For the day (6 am-6 pm) and night (7 pm-5 am) analyses, the dataset was split into day (148,654 data points) and night (175,682 data points) datasets. Then, the RH and T data for day and night were plotted in a correlation RHpT plot, with regression lines for day and night, yielding R^2 values of 0.15 and 0.08, respectively, as shown in Eqs. (2) and (3) (Fig. 5B). The R^2 values were very low for 37 years and day and night data. The decadal correlation analysis showed climate change in terms of changes in RH and T for New Delhi (Supplementary Fig. 2). Analysing all 37 years of data may not be the best approach for the RHpT plot, given the wide range of correlational changes, as evidenced by the low R^2 values. Further detailed seasonal analysis was conducted.

$$y = -1.18x + 73.43 \quad (1)$$

$$y = -0.99x + 62.36 \quad (2)$$

$$y = -0.79x + 68.96 \quad (3)$$

In the case of seasonal analysis, the 37 years of day and night data were divided into summer (April—September) and winter (October—March). The regression lines showed an improved relationship between RH and T, particularly during the day (Fig. 5C). The highest R^2 value (0.68) was observed for summer days, with a regression line as

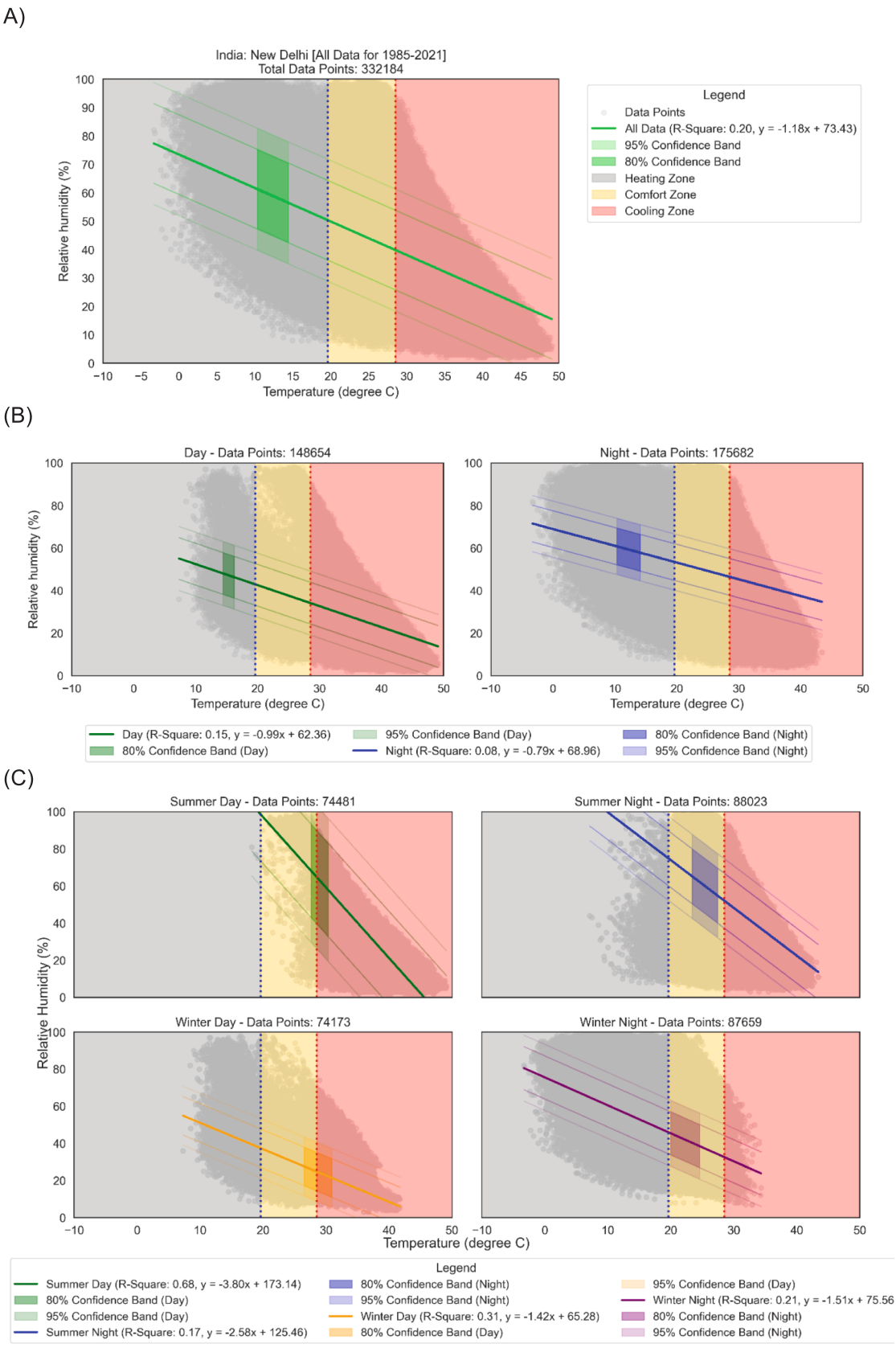

Fig. 5. RHpT plot for (A) all climate data, (B) day and night, (C) summer and winter day and night, and (D) monthly day and night for 1985–2021 from New Delhi, India.

described in Eq. (4), where the maximum data points fell within the cooling demand zone. The estimated regression line for summer nights

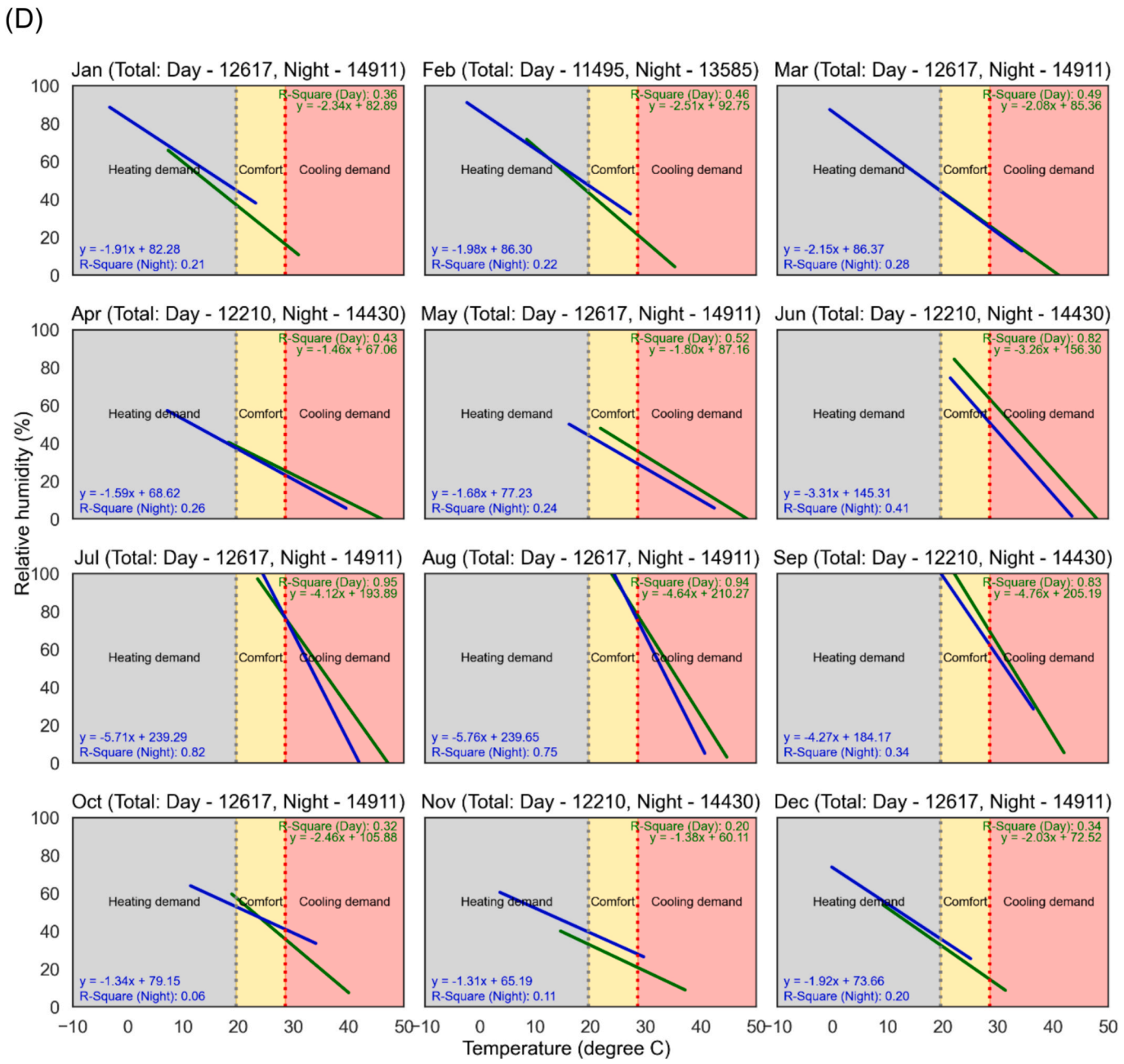

Fig. 5. (*continued*).

had an R^2 value of 0.17, as shown in Eq. (5). The R^2 value increased to 0.31 and then decreased to 0.21 for the regression lines with Eqs. (6) and (7), respectively, for the winter days and nights.

$$y = -3.80x + 173.14 \tag{4}$$

$$y = -2.58x + 125.46 \tag{5}$$

$$y = -1.42x + 65.28 \tag{6}$$

$$y = -1.51x + 75.56 \tag{7}$$

Monthly RHpT plots for day and night were developed to further analyse the relationship between RH and T. During the summer, the R^2 value was the highest. The monthly day analysis from April to September showed a significant increase in R^2 values (Fig. 5D) compared to the 37-year collective day analysis (Fig. 5C). In April, the R^2 value was 0.43, which increased to 0.52, 0.82, 0.95, 0.94 and 0.83 for the days in May-September, respectively. Also, the R^2 values were 0.46 and 0.49 in February and March (day), despite being considered as (late) winter. The R^2 value for the day was reduced to 0.32, 0.21, 0.34, and 0.36 in October, November, December, and January, respectively. The estimated regression lines for summer months for the day had Eq. (8), where A_{sd} was 1.46–4.76 and B_{sd} were 67.06–210.27, and for the winter months, the day had Eq. (9), where A_{wd} were 1.38–2.51 and B_{wd} were 60.11–105.88 (Fig. 5D).

$$y = -A_{sd}x + B_{sd} \tag{8}$$

$$y = -A_{wd}x + B_{wd} \tag{9}$$

The summer monthly night analysis from April to September also showed a significant increase in R^2 values (Fig. 5D) compared to the 37-year collective night analysis (Fig. 5C). In April, the R^2 value was 0.26,

which decreased to 0.24 in May before increasing to 0.41, 0.82, 0.75 and 0.34 for the nights in June-September, respectively. The R^2 value for winter monthly nights decreased to 0.06 in October and 0.11 in November. The R^2 value increased to 0.20, 0.21, 0.22 and 0.28 in December, January, February, and March, respectively. The estimated regression lines for summer months for the night had Eq. (10), where A_{sn} was 1.59–5.76 and B_{sn} were 68.62–239.65, and for winter months, for the night had Eq. (11), where A_{wn} were 1.31–2.15 and B_{wn} were 65.19–86.37 (Fig. 5D).

$$y = -A_{sn}x + B_{sn} \tag{10}$$

$$y = -A_{wn}x + B_{wn} \tag{11}$$

3.2. Translating RHpT into material thresholds

Wood is an abundant material with significant potential for architectural applications due to its moisture-responsive properties. For a responsive wood façade in New Delhi, the first step is to analyse the local humidity range. This analysis determines whether the wood's movement is sufficient to operate ventilation elements, such as night vents or panels, across various seasons and times of day. This analysis can be conducted using RHpT plots to characterise the material's behaviour under local climate conditions. For example, Fig. 6A (brown line) plots the complete humidity dataset for New Delhi from 1985 to 2021. If the design goal is for a wood-based vent to open at a high humidity level within the human comfort range (e.g., 40–50% RH), experimental testing should focus on that range. However, incorporating statistical confidence bands—such as 80% (purple dotted lines) or 95% (blue dotted lines)—would allow a designer to account for greater climatic variation. Using these bands, the operational RH range for experimental design could be expanded to 25–65% or 18–72%, respectively, making the system validated at lab and single-building simulation scales; further field testing is required against more extreme weather conditions.

In the case of Newcastle, materials could be employed to engineer passive and adaptive building façades during summer. However, if combined with passive heating, skin designs such as Trombe walls or

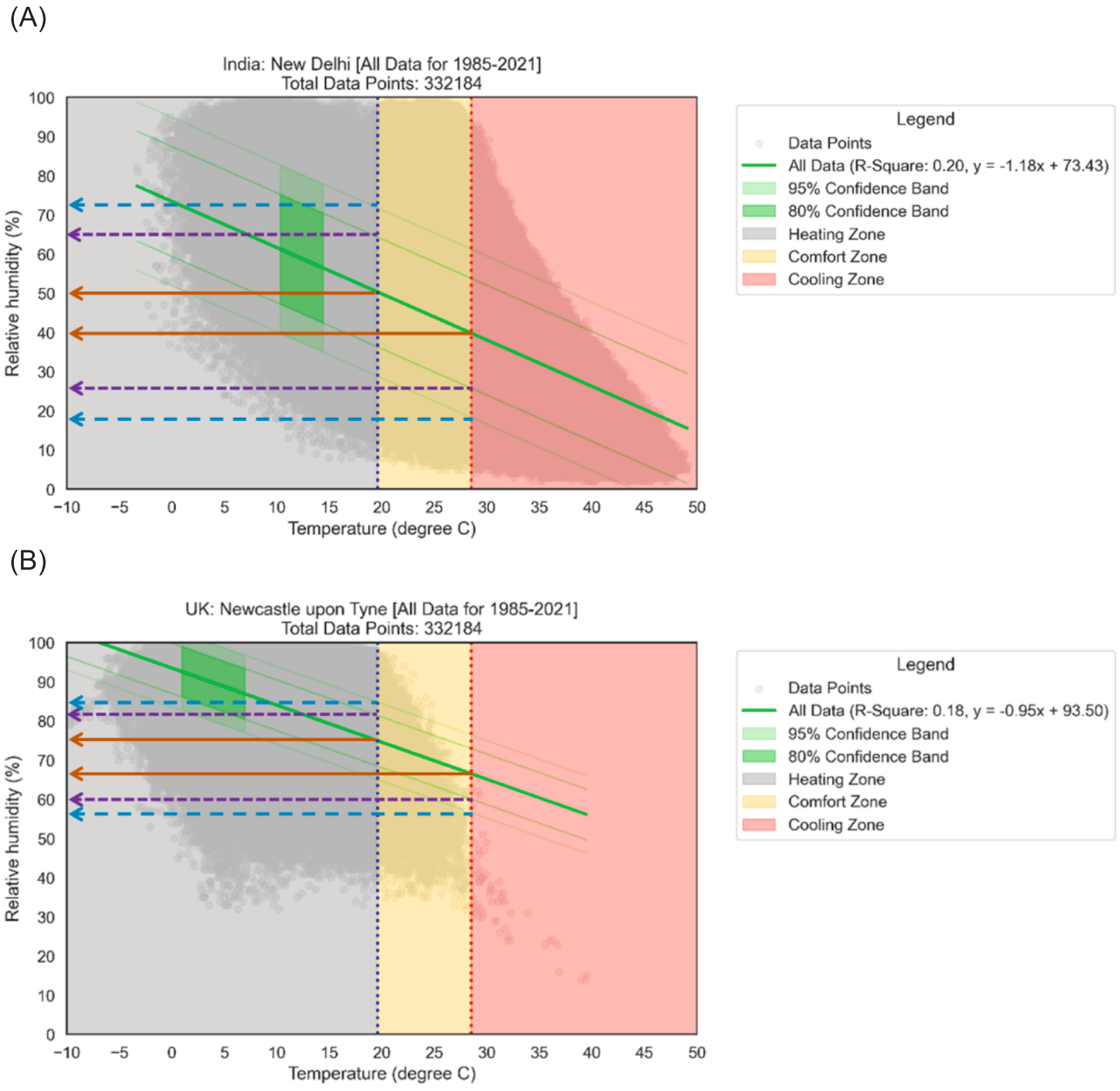

Fig. 6. Example of how RHpT plot could be used for (A) New Delhi and (B) Newcastle with lines of RH and T for the exploration range.

dynamic insulation, bio-based materials could be applied in Newcastle. As shown in Fig. 6B (brown line), considering only the whole dataset for 1985–2021, for example, if one would aim to design an adaptive/responsive vent or window with wood veneer or panels to be applied in the Trombe wall or dynamic insulation which they would want to open at high RH within comfort range, they would need to experiment within 65–75% RH range for operational use in Newcastle based on the RHpT plot. However, suppose they want to consider an 80% (purple dotted lines) or 95% (blue dotted lines) confidence band. In that case, they could design an experiment with the adaptive/responsive vent or window to be operational in 60–80% or 55–85% RH, respectively. These RH ranges would enable the exploration of various designs incorporating bio-based humidity-responsive materials within the operational range suitable for passive and adaptive building façades.

While this study focuses on two climatically divergent cities, this selective approach is instrumental as a proof-of-concept. The pronounced, year-round correlation in New Delhi (Cwa – humid subtropical) and the weaker, summer-only correlation in Newcastle (Cfb – marine west coast) serve as illustrative endmembers on a spectrum of potential climatic suitability. This comparison does not aim to provide a universally applicable rule, but rather to establish and validate the RHpT framework in two distinct contexts. It indicates that the method can differentiate between high and low-potential environments, providing a template for future analysis. The strong performance in New Delhi, a megacity facing extreme heat risks and rising cooling demands, is particularly significant for practical application. Ultimately, this work provides a validated methodological foundation for a larger-scale global analysis.

Periods identified as climatically unsuitable through the RHpT analysis—such as hot–humid daytime conditions or seasons with weak or inconsistent RH–temperature coupling—are explicitly treated as non-operational windows for humidity-responsive actuation. During these periods, hygromorphic apertures are assumed to remain in a passive fail-closed state, either due to insufficient humidity-driven deformation or through simple physical constraints embedded in the façade design. This inherent selectivity ensures that material actuation occurs only when it is likely to contribute positively to passive cooling or load reduction.

From a life-cycle perspective, this behaviour implies seasonal dormancy rather than continuous operation, consistent with other passive envelope strategies, such as night ventilation or solar shading. RHpT therefore functions as a screening framework that defines when humidity-responsive materials are appropriate, rather than prescribing year-round façade operation, thereby reducing the risk of adverse performance during unfavourable climatic conditions.

Despite the limitations of the climate and weather data (as mentioned in the Materials and methods section), RHpT plots can be derived from any other weather data, regardless of the data's timeframe. However, the amount of available data would affect the accuracy of the plots. Notably, weather data sourced from local weather stations is relevant and applicable for developing RHpT plots for subsequent use in examining and analysing the responsiveness of bio-based hygromorphic materials and systems within architectural contexts.

3.3. Establishing hygromorphic material thresholds

For New Delhi, the operational humidity thresholds for the responsive façade are fully defined as follows: the ventilation panel is closed at RH $< 40\%$, begins to open at RH $> 40\%$, and reaches its maximum displacement at RH $> 70\%$. This range (40–70% RH) was determined using the RHpT method, which showed strong statistical correlations with high R^2 values in our seasonal and diurnal analyses. It was selected because it lies entirely within the thermal comfort range for New Delhi. These thresholds were derived using linear regression models with 80% and 95% confidence intervals applied to 37 years of hourly weather data. This methodological approach ensured that the RH ranges selected for material testing served as reliable, location-specific proxies for temperature, thereby enhancing the method's reproducibility and transferability. (e.g., 40–70% for New Delhi), which directly informed the design and testing of the Bio-HNV (Bio-based Humidity-responsive Night Ventilation) system. Our material tests confirmed that larch veneers respond predictably within this RH range, and that their curvature response is both reversible and scalable. This close alignment illustrates the potential of the RHpT-derived humidity bands to be functionally meaningful for guiding material actuation.

A significant out-of-plane displacement from the wood veneer was observed in response to changes in RH. When the RH was increased from 20% to 50% and held for one hour, the centre of the panel deflected 6 mm out of plane. Increasing RH from 50% to 70%, the deflection increased to 9.5 mm within 1 h (Fig. 7B). The Bio-HNV structure deflects out-of-plane, generating spaces between the larch veneers (Fig. 7A), allowing air circulation through the screen under high RH. The 50–70% RH range corresponds closely to the RHpT-defined actuation zones for New Delhi, confirming the material's suitability for the local climate. These results provide the first empirical support for RHpT's role in informing material selection and façade performance design.

The deformation is reversible; when the RH is reduced, the woven veneer screen returns to its original position (Fig. 7C). However, the curing process is slower than the wetting process. Additionally, in the second cycle, both the sorption and desorption periods are prolonged, suggesting that larch veneers may exhibit reduced responsiveness to prolonged cyclic changes. The observed slower desorption response and partial decay in responsiveness over successive cycles highlight the importance of extended cyclic testing and ageing studies. This hysteretic behaviour further supports the use of conservative RH thresholds and seasonal dormancy strategies in façade design, rather than continuous actuation. Future work can therefore focus on long-term environmental exposure tests, accelerated ageing protocols, and façade-scale mock-ups to evaluate service life, maintenance requirements, and performance stability under realistic climatic and operational conditions.

Upon completion of the small-scale tests, the goal was to scale up the concept to form a larger structure that would benefit the research by ensuring the design and functionality of the large-scale prototype yield outputs similar to those of the small-scale one. A large-scale prototype was created (Fig. 7D), revealing that the thick larch strips follow a similar trend to the thin larch strips at the small scale. However, the thicker larch strips exhibit a higher deflection of approximately 12 mm, which can be attributed to the expanded span associated with the increased size of the upscaled larch veneer strips.

3.4. Night ventilation for low-tech cooling

This humidity-responsive character of the woven veneer structure was quantified and utilised to design different humidity-induced night ventilation solutions to assess the impact on indoor operative temperature, mechanical ventilation, and cooling demand in summer in New Delhi. Considering the Base case, scenarios 1 and 2 with different operational schedules (7 am, 8 am and 9 am), three selected dates in summer: April 1 (start of summer), July 1 (peak summer), and September 2 (end of summer), the initial simulation results showed a minor change in average operative temperature. The average operative temperature was 28 °C (April 1), 30.8 °C (July 1) and 30.7 °C (September 2) under the Base case, which fluctuated between −1 °C and 0.6 °C difference under Scenario 1 (Fig. 8) and 2 compared to the Base case, when the outdoor average temperatures were 28.9 °C (April 1), 32.9 °C (July 1), and 32.8 °C (September 2).

However, the significant impact of Bio-HNV-induced night ventilation on the total cooling energy demand was observed during the summer months (April 1-September 30). The total summer cooling energy demand was 9513.87 kWh. If the Bio-HNV were operational up to 7 am, it could reduce the total cooling energy demand by 0.64% and 1.46% under Scenarios 1 and 2, respectively, compared to the Base case. However, when the Bio-HNV was operational until 8 am, the total

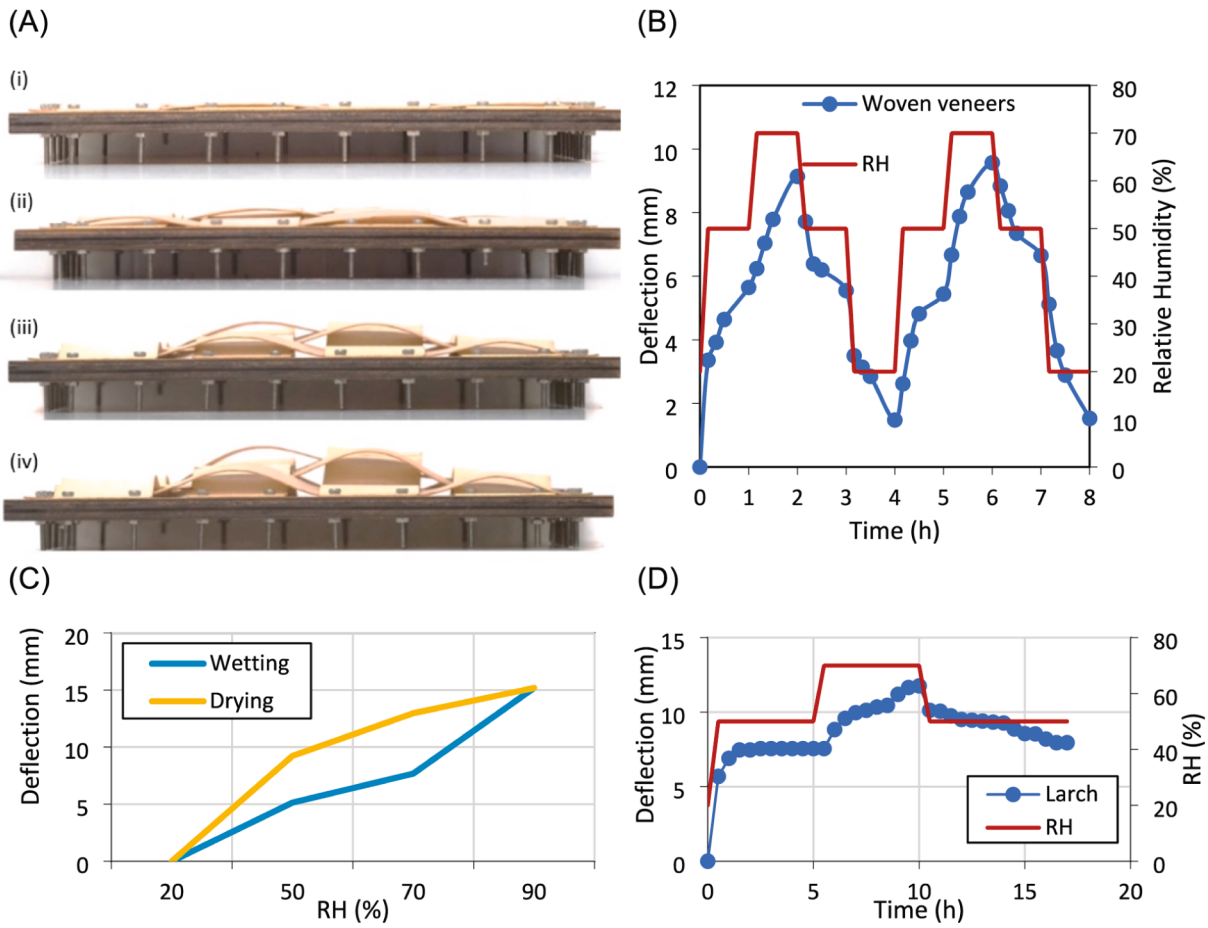

Fig. 7. (A) Humidity responsivity in Bio-HNV in RH (i) 20%, (ii) 50%, (iii) 70%, (iv) 90%. (B) Bio-HNV small-scale prototype – Cyclic behaviour between RH = 20%, 50%, 70%. (C) Hysteresis Curve of wood veneer swelling during one cyclic test at a constant temperature of 25 °C and different RH levels: 20%, 50%, 70% and 90%. (D) Bio-HNV large-scale prototype – Cyclic behaviour between RH = 20%, 50%, 70%.

cooling energy demand was reduced by 6.00% and 6.67% under Scenarios 1 and 2, respectively (Supplementary Fig. 4). The total cooling energy demand was reduced by 10.38% and 10.97% under Scenarios 1 and 2, respectively, compared to the base case, when Bio-HNV was operational until 9 am.

While the impact on average indoor operative temperature is modest, the primary benefit of the Bio-HNV system lies in reducing early-day mechanical cooling demand through passive night-time heat purging, highlighting a clear distinction between thermal comfort effects and energy performance outcomes under non-optimised conditions (south-facing façade, small openings, no cross-ventilation, and no insulation). Fig. 8 showed that the timing of night ventilation closing was critical, and that turning Bio-HNV's humidity responsiveness for the woven screen's opening and closing to specific humidity levels would be vital. Studies have shown that in India's hot-humid climatic context, cross-ventilation can enhance the effectiveness of night ventilation by increasing air circulation, improving ventilation strategies, optimising building orientation and shape, and considering wind speed and direction [45,46]. To enhance the effectiveness of Bio-HNV, further studies on cross ventilation, room proportions, internal insulation, outdoor shading, opening sizes, and wind to induce air movement need to be explored with fluid dynamics simulation and physical prototype testing to develop a functional and high-performance bio-based responsive night vent for climate resilience to extreme heat in New Delhi [1]. These modest performance improvements demonstrate the potential of using RHpT to guide façade actuation logic in hot-humid climates. They also illustrate how even simple, passive humidity-triggered systems can make meaningful contributions to climate resilience and energy efficiency.

RHpT does not imply that high relative humidity always corresponds to desirable opening conditions. Instead, it identifies specific temporal windows in which RH reliably covaries with temperature, allowing humidity to serve as a proxy for cooling-relevant thermal states. Outside these windows, the hygromorphic system remains inactive or closed, ensuring passive safety despite the absence of active control.

3.5. *Integration with building operation and practical constraints*

The humidity-responsive façade elements investigated in this study are not intended to operate continuously or universally, but rather during specific climatic windows identified through the RHpT screening process. During periods where outdoor conditions are unsuitable—such as hot–humid daytime conditions or extreme weather events—the system is assumed to remain in a passive fail-safe state, with apertures effectively closed. This seasonal and diurnal selectivity is a fundamental design feature rather than a limitation, ensuring robust operation despite the absence of active control systems.

In practical building applications, humidity-responsive façade elements would most likely be integrated into a hybrid envelope strategy. Their operation could be complemented by fixed or adjustable shading devices, night-time ventilation strategies, or conventional operable windows, allowing different passive mechanisms to dominate under different climatic conditions. In this context, hygromorphic apertures function as low-tech, self-regulating components that reduce cooling loads opportunistically rather than as stand-alone thermal control systems.

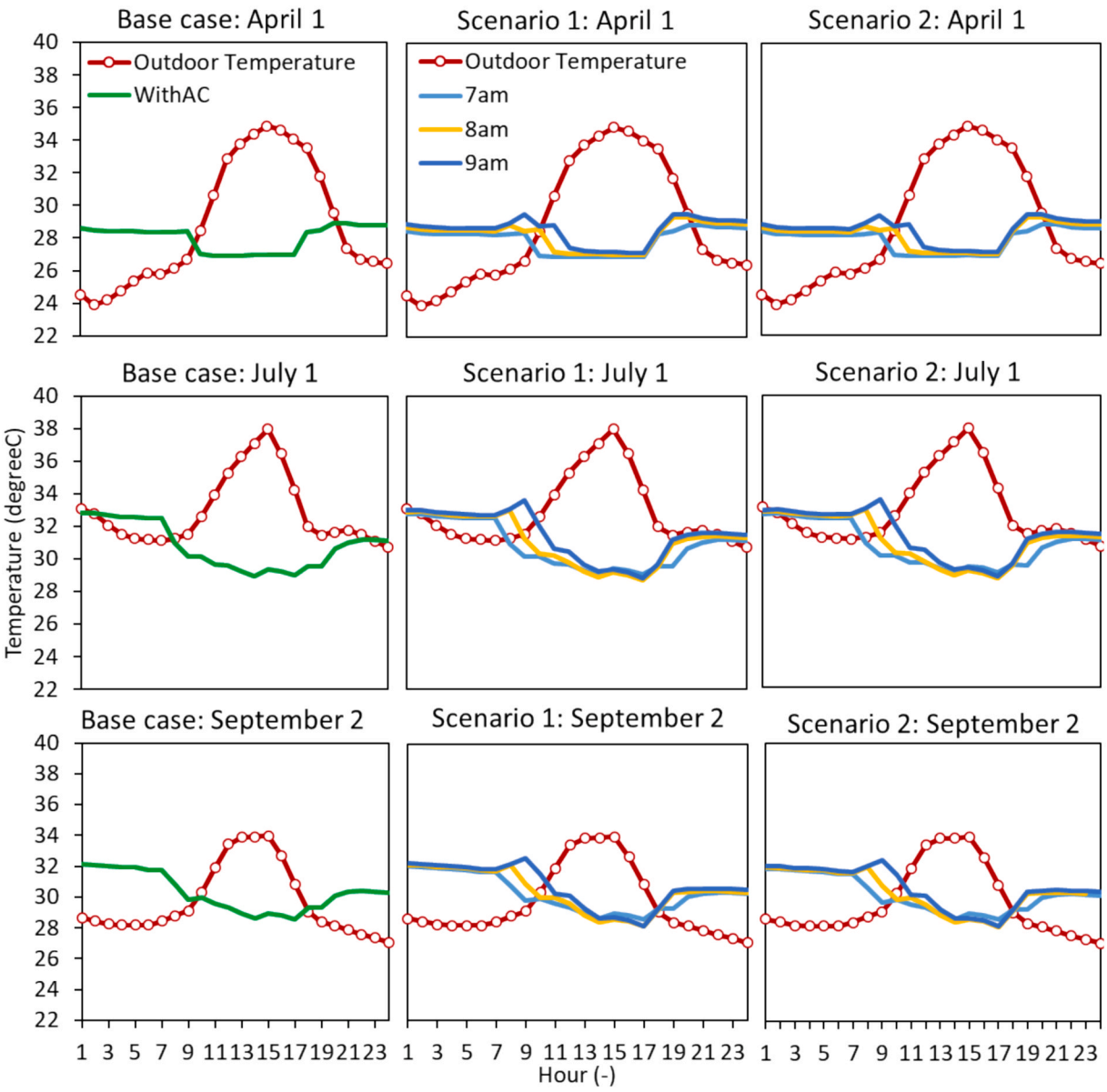

Fig. 8. Hourly indoor operative temperature on April 1, July 1 and September 2 under the Base case, Scenarios 1 and 2.

While the material response itself is autonomous, manual override or physical disablement during unfavourable seasons may be desirable in real buildings, particularly in retrofit scenarios. Such interventions could be undertaken through simple mechanical locking, removable panels, or seasonal maintenance protocols, without undermining the system's low-energy premise. Maintenance considerations primarily concern material ageing, biological degradation, and surface weathering, which are acknowledged as critical factors for long-term performance but fall outside the scope of the present proof-of-concept study.

3.6. Implications for urban policy and design

The RHpT framework extends beyond a technical design tool; it offers a new logic for urban climate adaptation policy that directly contributes to several UN Sustainable Development Goals (SDGs). For city planners and municipalities in hot-humid regions, RHpT can inform strategies that advance urban sustainability, equity, and resilience:

- **SDG 11 (Sustainable Cities and Communities) & SDG 13 (Climate Action):** RHpT enables urban climate zoning maps that identify neighbourhoods with high potential for passive humidity-responsive façades. This allows for targeted retrofit programs that prioritise areas where the climate correlation is strongest and the social need is greatest—such as social housing, public schools, and informal settlements—simultaneously reducing urban energy demand (SDG 7) and mitigating the urban heat island effect.
- **SDG 12 (Responsible Consumption and Production) & SDG 9 (Industry, Innovation and Infrastructure):** The framework supports the development of open-access, city-specific material databases that match local RHpT-derived humidity bands to validated, locally sourced bio-based materials. This fosters circular bio-economies, reduces embodied carbon in the construction sector, and stimulates innovation in local material supply chains.
- **SDG 7 (Affordable and Clean Energy) & SDG 11:** RHpT provides the empirical basis for moving beyond prescriptive building codes to performance-based standards that reward passive, climate-responsive design. By incentivising building skins that adapt to their environments without external energy input, cities can lock in long-term reductions in cooling energy consumption.

While the current study employs a simplified model, it provides critical proof-of-concept. The next step is to test these systems at the district scale, integrating urban variables such as wind patterns, density, and socio-economic data to validate their contribution to city-wide resilience and equitable climate goals (SDG 10).

While the present study demonstrates the feasibility of RHpT-guided humidity-responsive façades at the individual building scale, extending this approach to the district or city scale introduces additional complexities. At the building scale, material actuation is primarily governed by local ambient humidity and façade-level airflow, making implementation feasible within existing retrofit practices.

At larger spatial scales, however, the performance of humidity-responsive systems would be influenced by coupled effects, including urban morphology, street-level airflow, building density, and interactions among multiple ventilated façades. These factors may alter local humidity and temperature patterns, requiring integration with urban climate modelling, computational fluid dynamics (CFD), and district-scale energy simulations. Accordingly, while RHpT provides a robust screening framework for identifying climatic suitability, its application at district and city scales should be understood as a future research direction rather than an immediate design prescription.

Beyond historical climate analysis, the RHpT framework can also be directly extended to future climate projections using downscaled Coupled Model Intercomparison Project (CMIP) or ERA5-based scenario data. This would enable designers and policymakers to assess how the temporal reliability of humidity-driven actuation may shift under climate change, supporting future-proof façade strategies and long-term adaptation planning in rapidly warming urban regions.

4. Conclusion: Toward equitable, circular, and climate-responsive design

This work advances a new logic for urban climate adaptation—one grounded in ecological materials, bioclimatic analysis, and spatial justice. The RHpT framework transforms long-term urban climate data into actionable design thresholds, providing a globally scalable yet locally tunable tool for passive, sensor-free building adaptation. Our findings show that in high-potential climates such as New Delhi, bio-façades guided by RHpT can reduce cooling energy demand, offering a viable pathway for low-carbon resilience. The cooling energy reductions reported here should be interpreted as conservative, proof-of-concept indicators derived from a simplified, non-optimised building model, rather than as validated performance predictions for full-scale deployment.

Critically, this approach directly addresses urban equity gaps. By leveraging local climate patterns and abundant bio-based materials, it provides an accessible, low-tech alternative to energy-intensive innovative systems for residents in the Global South who lack access to mechanical cooling. Beyond the specific Bio-HNV prototype, the RHpT method serves as a transferable framework, enabling cities to identify climatic opportunities for passive actuation, evaluate material suitability, and prioritise retrofit strategies within broader adaptation plans.

While demonstrated here in two contrasting urban contexts, the framework is transferable to other cities and megacities and could be extended to projected climate scenarios to support future-proof planning. The cooling reductions reported are a conservative baseline; larger gains are expected when RHpT façades are integrated with cross-ventilation, shading, and hybrid systems. Addressing the durability and field performance of hygromorphic materials remains an important next step; yet the principle is clear: by harnessing the inherent properties of bio-based materials, urban areas can expand their repertoire of equitable, low-carbon adaptation strategies. Finally, this study lays the groundwork for a paradigm shift toward adaptive urban buildings that work in concert with their local environment, fostering localised resilience that is not only sustainable but also just.

CRediT authorship contribution statement

Kumar Biswajit Debnath: Writing – review & editing, Writing – original draft, Visualization, Validation, Software, Resources, Methodology, Investigation, Formal analysis, Data curation, Conceptualization. **Natalia Pynirtzi:** Writing – review & editing, Writing – original draft, Visualization, Validation, Methodology, Investigation, Formal analysis, Data curation, Conceptualization. **Jane Scott:** Writing – review & editing, Supervision, Project administration, Funding acquisition. **Colin Davie:** Supervision. **Ben Bridgens:** Writing – review & editing, Writing – original draft, Supervision, Project administration, Funding acquisition.

Declaration of competing interest

The authors declare that they have no known competing financial interests or personal relationships that could have appeared to influence the work reported in this paper.

Acknowledgements

This research was funded by the 'RESPIRE: Passive, Responsive, Variable Porosity Building Skins' project (ID/Ref: 91782), which is funded by The Leverhulme Trust. We would like to thank Meteoblue (www.meteoblue.com) for its collaboration on climate data. This work was also supported by the Chancellor's Research Fellowship (CRF), funded by the University of Technology Sydney (UTS), Sydney, Australia.

Appendix A. Supplementary data

Supplementary data to this article can be found online at https://doi.org/10.1016/j.enbuild.2026.117192.

Data availability

The authors do not have permission to share data.

References

[1] K. B. Debnath, D. Jenkins, S. Patidar, A. D. Peacock and B. Bridgens, "Climate change, extreme heat, and South Asian megacities: Impact of heat stress on inhabitants and their productivity," *ASME Journal of Engineering for Sustainable Buildings and Cities,* vol. 4, no. 4, 2023. https://doi.org/10.1115/1.406402.

[2] IPCC, Climate Change 2023: Synthesis Report. Contribution of Working Groups I, II and III to the Sixth Assessment Report of the Intergovernmental Panel on Climate Change, Intergovernmental Panel on Climate Change, 2023.

[3] K.B. Debnath, O. Osunmuyiwa, D.P. Jenkins, A.D. Peacock, A mixed-methods approach for evaluating the influence of residential practices for thermal comfort on electricity consumption in Auroville, India, Electricity 5 (1) (2024) 112–133.

[4] K.B. Debnath, D.P. Jenkins, S. Patidar, A.D. Peacock, Understanding residential occupant cooling behaviour through electricity consumption in warm-humid climate, Buildings 10 (4) (2020) 78.

[5] K.B. Debnath, M. Mourshed, Challenges and gaps for energy planning models in the developing-world context, Nat. Energy 3 (3) (2018) 172–184.

[6] R. Aslanoğlu, J.K. Kazak, S. Szewrański, M. Świąder, G. Arciniegas, G. Chrobak, A. Jakóbiak, E. Turhan, Ten questions concerning the role of urban greenery in shaping the future of urban areas, Build. Environ. 267 (2025) 112154.

[7] F. Yousefi, F. Nocera, The role of Ab-anbars in the vernacular architecture of iran with emphasis on the performance of wind-catchers in hot and dry climates, Heritage 4 (4) (2021) 3987–4000.

[8] Z.S. Zomorodian, M. Tahsildoost, Energy and carbon analysis of double skin façades in the hot and dry climate, J. Clean. Prod. 197 (2018) 85–96.

[9] H.S.M. Shahin, Adaptive building envelopes of multistory buildings as an example of high performance building skins, Alex. Eng. J. 58 (1) (2019) 345–352.

[10] M. Sobczyk, S. Wiesenhütter, J.R. Noennig, T. Wallmersperger, Smart materials in architecture for actuator and sensor applications: a review, J. Intell. Mater. Syst. Struct. 33 (3) (2022) 379–399.

[11] K.B. Debnath, N. Pynirtzi, J. Scott, C. Davie, B. Bridgens, Bio-jaali: Reimagining vernacular passive cooling screens with mycelium-based composites, Energy and Buildings (2026) 117104, https://doi.org/10.1016/j.enbuild.2026.117104.

[12] M.H. Ramage, H. Burridge, M. Busse-Wicher, G. Fereday, T. Reynolds, D.U. Shah, G. Wu, L. Yu, P. Fleming, D. Densley-Tingley, J. Allwood, P. Dupree, P.F. Linden,

O. Scherman, The wood from the trees: the use of timber in construction, Renew. Sustain. Energy Rev. 68 (2017) 333–359.
[13] G. Wimmers, Wood: a construction material for tall buildings, Nat. Rev. Mater. 2 (12) (2017) 1–2.
[14] J. Hildebrandt, N. Hagemann, D. Thrän, The contribution of wood-based construction materials for leveraging a low carbon building sector in Europe, Sustain. Cities Soc. 34 (2017) 405–418.
[15] N. Pynirtzi, K. B. Debnath, G. Lantzanakis, K. Bloch, J. Scott, C. Davie and B. Bridgens, "Evaluating the Humidity Responsiveness of Bacterial Cellulose for Application in Responsive, Breathable Building Skins," in *International Conference on Bio-Based Building Materials. ICBBM 2023. RILEM Bookseries*, 2023. https://doi.org/10.1007/978-3-031-33465-8_49.
[16] M. Jones, A. Mautner, S. Luenco, A. Bismarck, S. John, Engineered mycelium composite construction materials from fungal biorefineries: a critical review, Mater. Des. 187 (2020) 108397.
[17] D. Raslan, E. Elsacker, K.B. Debnath, M. Dade-Robertson, The role of surface interventions in bio-welding mycelium based-composites, Sustain. Mater. Technol. (2025) e01326.
[18] A. Holstov, B. Bridgens, G. Farmer, Hygromorphic materials for sustainable responsive architecture, Constr. Build. Mater. 98 (2015) 570–582.
[19] S. Reichert, A. Menges, D. Correa, Meteorosensitive architecture: Biomimetic building skins based on materially embedded and hygroscopically enabled responsiveness, Comput. Aided Des. 60 (2015) 50–69.
[20] M. Rüggeberg, I. Burgert, Bio-inspired wooden actuators for large scale applications, PLoS One 10 (4) (2015) e0120718.
[21] A. Menges, S. Reichert, Performative wood: physically programming the responsive architecture of the hygroscope and hygroskin projects, Archit. Des. 85 (5) (2015) 66–73.
[22] D.M. Wood, D. Correa, O.D. Krieg, A. Menges, Material computation—4D timber construction: Towards building-scale hygroscopic actuated, self-constructing timber surfaces, Int. J. Archit. Comput. 14 (1) (2016) 49–62.
[23] S. Poppinga, C. Zollfrank, O. Prucker, J. Rühe, A. Menges, T. Cheng, T. Speck, Toward a new generation of smart biomimetic actuators for architecture, Adv. Mater. 30 (19) (2018) 1703653.
[24] P. Grönquist, F. Wittel, M. Rüggeberg, Modeling and design of thin bending wooden bilayers, PLoS One 13 (10) (2018) e0205607.
[25] C. Vailati, E. Bachtiar, P. Hass, I. Burgert, R. Markus, An autonomous shading system based on coupled wood bilayer elements, Energy Build. 158 (2018) 1013–1022.
[26] P. Grönquist, D. Wood, M.M. Hassani, F.K. Wittel, A. Menges, M. Rüggeberg, Analysis of hygroscopic self-shaping wood at large scale for curved mass timber structures, Sci. Adv. 5 (9) (2019) eaax1311.
[27] G. Pelliccia, G. Baldinelli, F. Bianconi, M. Filippucci, M. Fioravanti, G. Goli, A. Rotili, M. Togni, Characterisation of wood hygromorphic panels for relative humidity passive control, J. Build. Eng. 32 (2020) 101829.
[28] P. Grönquist, P. Panchadcharam, D. Wood, A. Menges, M. Rüggeberg, F.K. Wittel, Computational analysis of hygromorphic self-shaping wood gridshell structures, R. Soc. Open Sci. 7 (7) (2020) 192210.
[29] R. El-Dabaa, S. Abdelmohsen, Y. Mansour, Programmable passive actuation for adaptive building façade design using hygroscopic properties of wood, Wood Mat. Sci. Eng. 16 (4) (2021) 246–259.
[30] V. Olgyay, Design with climate: bioclimatic approach to architectural regionalism, Princeton, Princeton University Press, New Jersey, 2015.
[31] M. Hensel, A. Menges, M. Weinstock, Emergent technologies and design: towards a biological paradigm for architecture, Oxfordshire, England, Routledge, UK, 2013.
[32] S. Chatterjee, P.-C.-L. Hui, Review of applications and future prospects of stimuli-responsive hydrogel based on thermo-responsive biopolymers in drug delivery systems, Polymers 13 (13) (2021) 2086.
[33] V. Gopinath, S. Saravanan, A. Al-Maleki, M. Ramesh, J. Vadivelu, A review of natural polysaccharides for drug delivery applications: special focus on cellulose, starch and glycogen, Biomed. Pharmacother. 107 (2018) 96–108.
[34] B. Das, M. Mandal, A. Upadhyay, P. Chattopadhyay, N. Karak, Bio-based hyperbranched polyurethane/Fe3O4 nanocomposites: smart antibacterial biomaterials for biomedical devices and implants, Biomed. Mater. 8 (3) (2013) 035003.
[35] A. Menges, Material resourcefulness: activating material information in computational design, Archit. Des. 82 (2) (2012) 34–43.
[36] D. Wood, C. Vailati, A. Menges, M. Rüggeberg, Hygroscopically actuated wood elements for weather responsive and self-forming building parts–Facilitating upscaling and complex shape changes, Constr. Build. Mater. 165 (2018) 782–791.
[37] H.E. Beck, N.E. Zimmermann, T.R. McVicar, N. Vergopolan, A. Berg, E.F. Wood, Present and future Köppen-Geiger climate classification maps at 1-km resolution, Sci. Data 5 (1) (2018) 180214.
[38] Climate.OneBuilding, "Repository of free climate data for building performance simulation," 12 September 2022. [Online]. Available: https://climate.onebuilding.org/default.html. [Accessed 15 January 2023].
[39] Meteoblue, "Datasets," Meteoblue, 9 May 2023. [Online]. Available: https://docs.meteoblue.com/en/meteo/data-sources/datasets#era5-era5t. [Accessed 08 August 2023].
[40] OPEX, "Interpreting the Pearson Coefficient," OPEX Resources, 13 October 2017. [Online]. Available: https://opexresources.com/interpreting-pearson-coefficient/#:~:text=The%20Pearson%20coefficient%20helps%20to,be%20interpreted%20together%2C%20not%20individually.. [Accessed 05 April 2023].
[41] ECMWF, "ERA5: data documentation," European Centre for Medium-Range Weather Forecasts, 30 October 2023. [Online]. Available: https://confluence.ecmwf.int/display/CKB/ERA5%3A+data+documentation#ERA5:datadocumentation-Accuracyanduncertainty. [Accessed 01 November 2023].
[42] ECMWF, "ERA5: uncertainty estimation," European Centre for Medium-Range Weather Forecasts, 05 May 2023. [Online]. Available: https://confluence.ecmwf.int/display/CKB/ERA5%3A+uncertainty+estimation#ERA5:uncertaintyestimation-(6)HowreliableistheERA5uncertaintyestimate?. [Accessed 01 November 2023].
[43] S. Manu, Y. Shukla, R. Rawal, L.E. Thomas, R. De Dear, Field studies of thermal comfort across multiple climate zones for the subcontinent: India Model for Adaptive Comfort (IMAC), Build. Environ. 98 (2016) 55–70.
[44] R. J. Ross and others, "Wood handbook: wood as an engineering material," USDA Forest Service, Forest Products Laboratory, General Technical Report FPL- GTR-190, 2010: 509 p. 1 v., Forest Products Laboratory, 2010.
[45] R. Stasi, F. Ruggiero, U. Berardi, Influence of cross-ventilation cooling potential on thermal comfort in high-rise buildings in a hot and humid climate, Build. Environ. 248 (2024) 111096.
[46] M. Prabhakar, M. Saffari, A. de Gracia, L.F. Cabeza, Improving the energy efficiency of passive PCM system using controlled natural ventilation, Energy Build. 228 (2020) 110483.